High Resolution Charge Measurements of UH Cosmic Ray Nuclei Using a Direct Imaging Cherenkov Ground-based Observatory

D. Kieda[a**], S.P Swordy[b], S.P. Wakely[b] and A. Virshup[c]

[a]Utah High Energy Astrophysics Institute, University of Utah;
[b]Enrico Fermi Institute, University of Chicago
[c]Grinnell College

ABSTRACT

The accurate determination of the elemental composition of cosmic rays at high energies is expected to provide crucial clues on the origin of these particles. Here we discuss a technique that has become possible through the use of modern ground-based Cherenkov imaging detectors. We combine a measurement of the Cherenkov light produced by the incoming cosmic-ray nucleus in the upper atmosphere with an estimate of the total nucleus energy produced by the extensive air shower initiated when the particle interacts deeper in the atmosphere. The emission regions prior to and after the first nuclear interaction can be separated by an imaging Cherenkov system with sufficient angular and temporal resolution. Monte Carlo simulations indicate a widely space array of 10m diameter imaging Cherenkov detectors should have charge resolution of $\Delta Z/Z$ <5% for incident iron nuclei in the region of the ``knee" of the cosmic-ray energy spectrum. This technique also has the intriguing possibility to unambiguously discover nuclei heavier than iron at energies above 10^{14} eV. We describe a strawman detector design for a future observatory dedicated to high resolution cosmic ray measurements. This observatory can also serve as a wide field of view TeV gamma-ray survey instrument.

Keywords: Cosmic Ray; Cherenkov Light; gamma-ray astronomy; measurement techniques; quark star; UH nuclei; magnetic monopole

1. Introduction

The origin of cosmic rays remains a central unresolved question in astrophysics. Nearly 90 years after the first observations, this population of charged particles remains an enigma; the heart of which is the huge dynamic range of fluxes and energies over which they have been observed. In the theoretical arena, a relatively recent paradigm has emerged, which involves the acceleration of cosmic rays via diffusive shock processes in supernovae remnants (SNR). This idea has been fueled both by a viable physical model of the acceleration process[1,2,3,4] and a simple energetics argument in which galactic supernovae are the only galactic candidate with sufficient energy output to supply the staggering amount of power needed to sustain the cosmic-ray population[5].

A key issue with the SNR idea is that supernova diffusive shock acceleration can only produce particles up to some maximum energy, limited either by the lifetime of the strong shock or by the particles becoming so energetic they can no longer be confined in the acceleration region[6]. Estimates of this upper energy limit vary, with typical values in the region of 100 TeV (1 TeV = 10^{12} eV). However, the observed flux of cosmic rays extends more or less continuously for another five orders of magnitude beyond this; no plausible extrapolation of the standard parameters of SNR can generate cosmic rays of these energies.

Another aspect of the cosmic ray riddle is the existence of an observational ``knee" at ~ $10^{15}$ eV in the cosmic ray energy spectrum (Figure 1). The coincidence of this ``knee" with the theoretical energy limit of SNR diffusive shock acceleration is intriguing and has actually served as evidence to support the theory. However the ``knee" represents only a small change in the spectral slope of the overall flux, with the energy dependence changing from $E^{-2.75}$ below the ``knee" to $E^{-3.0}$ above it. We are faced with a simple observational fact that the cosmic rays have an essentially continuous spectral slope for nearly 11 orders of magnitude.

** Presenting Author

Particle Astrophysics Instrumentation, Peter W. Gorham, Editor,
Proceedings of SPIE Vol. 4858 (2003) © 2003 SPIE · 0277-786X/03/$15.00

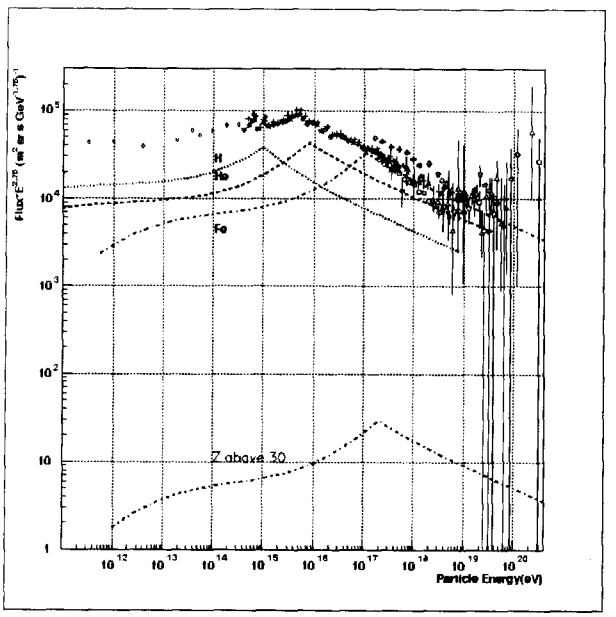

Figure 1: Knee in all particle cosmic ray energy spectrum, and Ultra Heavy (Z>30) cosmic ray primary flux extrapolated from HEAO-3 satellite measurements[13] to the PeV energy range using a leaky-box propagation model[14]. Horizontal Axis: Primary cosmic energy (eV). Vertical Axis: Differential Cosmic Ray flux multiplied by $E^{2.75}$. Individual points: All particle flux measurements from various experiments.

In principle, additional mechanisms could provide the flux at high energies. The power budget for ``post-knee'' cosmic rays is only a fraction that of the total budget, so there is some freedom in selecting models. However, to result in an energy spectrum as smooth as observed, these mechanisms would have to generate fluxes that are remarkably close to that of the SNR mechanism.

An overall scheme that credibly addresses and unifies these issues remains elusive. More reliable and accurate measurements in the ``knee'' region, of abundant cosmic ray nuclei (1 < charge Z < 26) could drastically revise our current ideas and provide a basis for such a unification. The accurate determination of the composition of cosmic rays has provided some of the key advances in this field at lower energies, where direct measurements are possible with detectors above the atmosphere. For example, the realization that the observed spectral slope[7] of cosmic rays is significantly steeper than that produced in the cosmic ray sources themselves resulted from measurements with sufficient elemental resolution to separate primary source cosmic ray elements from those produced in the interstellar medium at 10^{11} eV .

In this paper we describe the capabilities of a new high resolution technique based on the concept that a detector of fine enough pixellation will be capable of observing Cherenkov light emitted directly from cosmic ray nuclei prior to their first interaction in the atmosphere[8] (Figure 2). In previous atmospheric Cherenkov observatories, this light is overwhelmed by the Cherenkov emission from the subsequent extensive air shower (EAS). However, with an appropriate detector, and within certain geometric constraints, this ``direct Cherenkov'' light, or DC light, light can be sufficiently well separated from the background of EAS Cherenkov light to make relatively high-precision measurements of the traditional cosmic ray composition (1 < Z < 26). which may possess key information for understanding the origin of cosmic rays beyond the knee.

2. Direct Cherenkov Light signature in Atmospheric EAS

The targeting of DC light is not a new idea. In 1965, Sitte[9] proposed that this radiation might be observed by high-altitude balloon-borne optical telescopes. His idea (revisited by Gough[10] in 1976) was to place optical detectors at a height in the atmosphere above the mean interaction point of heavy primary cosmic rays and to look for the direct production of Cherenkov light. In the absence of the large light backgrounds due to emission from EAS, it was expected that accurate composition measurements could be made by analysis of the DC light yields. After a pioneering flight by Sood[11] in 1981, the concept was unexploited until recent efforts[12] in 1998. The fundamental challenge in the new approach discussed here is the identification of the DC light against the much larger background of Cherenkov light produced in the associated EAS.

Since the dominant background for the DC light is Cherenkov light from electrons scattered in the EAS development, we have used numerical simulations to study the levels and fluctuations in this background. The characteristics of DC light in EAS have been modeled using a modified MOCCA Monte Carlo Simulation[15,16,17] and also the CORSIKA (Version 5.945, QGSJet98) simulation package[18].

Figure 3 illustrates the angular and time characteristics of DC light emitted by a single 100 TeV vertical iron cosmic ray which interacts and produces an EAS deeper in the atmosphere. The time axis corresponds to the time delay compared to

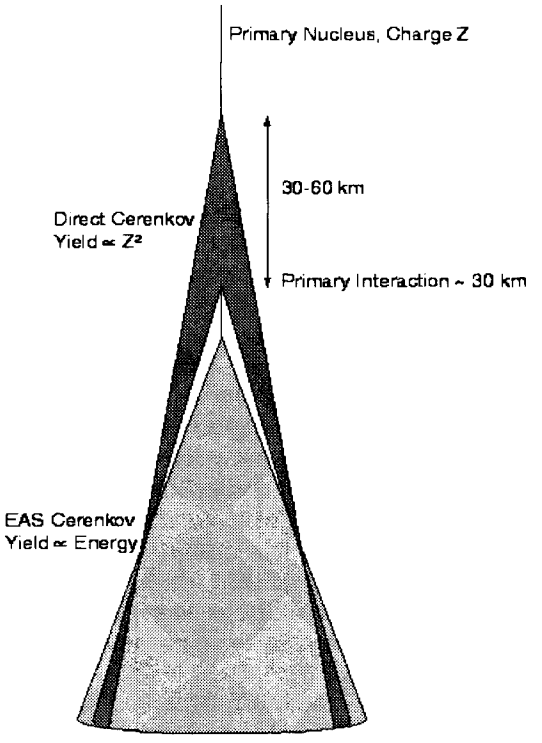

Figure 2: Schematic depiction of Direct Cherenkov (DC) Light emission by primary cosmic ray nucleus. DC light is emitted by the primary cosmic ray at high altitudes, before the first nuclear interaction of the primary with the atmosphere.

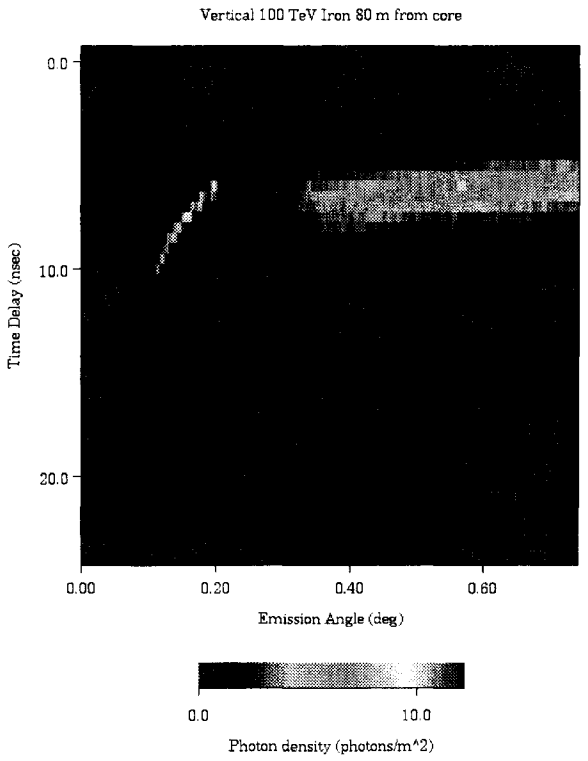

Figure 3: Direct and EAS Cherenkov light emitted from 100 TeV iron nucleus with a vertical trajectory. The Cherenkov light is observed at a mean radius of 80 m from the shower axis. Multiple scattering of the Cherenkov light due to Rayleigh and Mie scattering from a wind-driven aerosol model[19] of the atmosphere is included. The vertical axis is the time delay of the arriving photons as discussed in the text. The horizontal axis is the arrival angle of the photons with respect to the vertical at the observing site. The scales below each panel give the photon intensities.

a reference arrival time at sea level of a particle traveling at a vacuum speed of light c along the incoming nucleus path. The angular axis corresponds to the angle of entry of the photons into the detector compared to the incoming particle trajectory. The photon density of the light is averaged over an annulus extending from 67 m to 94 m from the shower axis, giving an 80m mean radius of the annulus, and the intensity is integrated over a wavelength band of 300-600 nm, as observed at sea level. Multiple scattering of Cherenkov is simulated using the LOWTRAN standard wind-driven aerosol model of Mie and Rayleigh scattering processes[19]. The DC light emission is clearly seen as an arc on the left of the figure, separated from the Cherenkov emission produced by the EAS.

The DC light technique can only be exploited over a limited energy window. The lower energy threshold is defined by the Lorentz velocity threshold for Cherenkov emission, while the upper energy threshold is determined by the energy at which the secondary EAS Cherenkov light overwhelms the DC light. This window expands like ~Z for heavy nuclei (Figure 4). A DC measurement of Iron nuclei (Z=26) is possible into the cosmic-ray ``knee" region, around 1000 TeV.

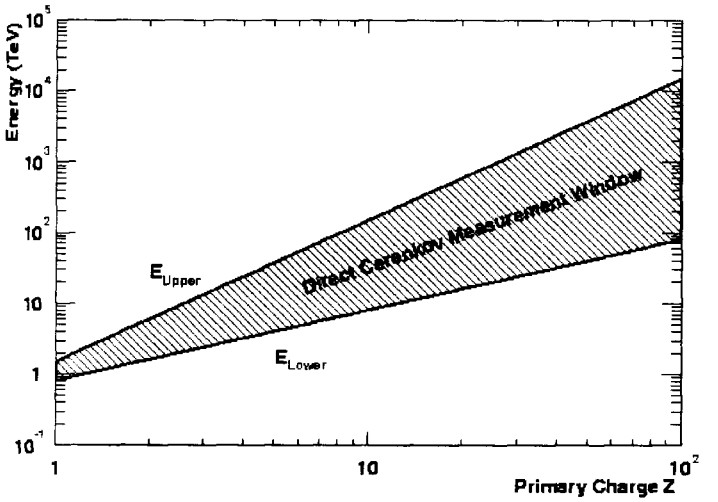

Figure 4: Energy window for Observation window for DC light as a function of Primary charge Z.

3. A Direct Cherenkov Observatory (DCO)

3.1. Strawman Design

A conceptual DCO design uses a number of large (>10 m diameter) telescopes located on fixed, vertical pointing mounts. The telescopes are separated by a distance of approximately 80 m (Figure 5). Each telescope consists of a 10 m diameter, wide field-of-view optical concentrator, a highly pixellated focal plane, and a photomultiplier readout plane (Figure 6). In the preferred implementation, the optical concentrator provides an isochronous surface to preserve the incoming wavefront timing to approximately 2 ns or better. This timing requirement provides additional separation between the DC light and the secondary Cherenkov light. Possible optical concentrators include multiple UV transmitting Fresnel lenses currently being developed for the OWL satellite observatory[20]. Simulations of these optical systems indicate excellent imaging capabilities out to fields of view or 45° or more.

A highly pixellated focal plane images the Cherenkov light from the cosmic ray shower. In order to have sufficient resolution and signal-to-noise ratio for DC light measurement, small pixels (0.1°) are necessary. For a 45° field of view camera, one would require more than 10^5 pixels to image the entire field of view. In order to reduce costs, the individual pixels in the focal plane are optically multiplexed into a secondary optical readout plane which employs multi-anode photomultiplier tubes (Figure 6). Monte Carlo simulations of optically or electronically multiplexed signals (Figures 7 and 8) indicate a pixel undersampling by factors of 6 can be accommodated, at a cost of increased background light per photomultiplier tube pixel as well as increased optical loss. This will result in a commensurate increase in the energy threshold of the instrument. However, for observations of high-Z PeV cosmic rays, these compromises are acceptable.

Light striking the individual pixels is read out by a fast FADC system, with 500 MHz sampling rate or faster, enabling an image to be constructed in time versus/angle like those shown in Figure 3. A key advantage of the DC method over the observations of Cherenkov light high in the atmosphere is that the triggering of the system is relatively simple. Since a significant part of the EAS will develop in the field of view of the telescopes, this large light signal can be used to provide a simple trigger scheme. A Cherenkov light signal produced by an EAS with energies > 10 TeV can be reliably discriminated from the night sky by simple logic on the camera pixels for a 10 m mirror size. Using individual-tube constant fraction discriminators, hit patterns from multiple pixels are combined using fast logic tables to look for sequences of pixels with characteristics similar to a Cherenkov image. Once a mirror is triggered, it retrieves a history of photon time slices from the FADC system for about 20-50 nanoseconds around the trigger time to look for the delayed DC light signal. Neighboring telescopes in the array would also be read out to look for coincidence measurement of the same Cherenkov image from different observation angles. The data from multiple telescopes is combined to determine the shower geometry, energy, and DC light content. Importantly, events can be required to contain consistent amounts of DC light intensity and location in multiple telescopes. This procedure can reject essentially all light signal contamination from local sources, for example local muons, and verify the level of DC emission from independent measurements.

The total detection aperture is not only affected by the physical size of the observatory and the field of view of each camera; it is also affected by additional constraints needed to observe the DC, light such as requiring the shower core to strike in an annulus between 50-115 m from the individual detectors. Because we are using an array of multiple telescopes, in general the shower core will fall within an acceptable distance from more than one telescope over most of

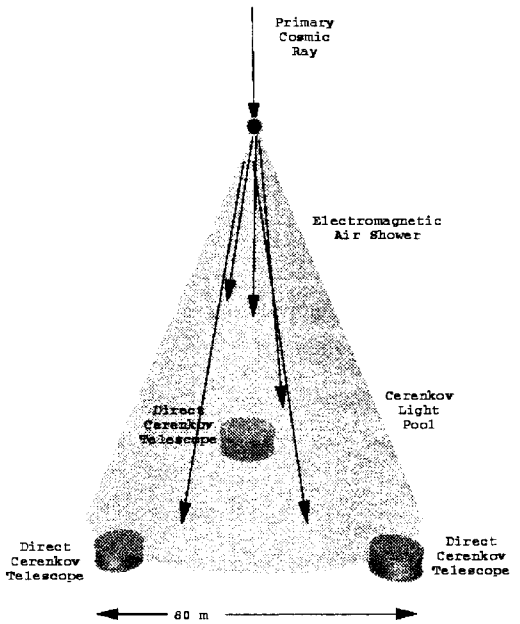

Figure 5: Conceptual Direct Cherenkov Observatory Strawman design. Each wide field of view (45-60°) DCO telescope observes the Cherenkov light pool from the cosmic ray air shower with 0.1° pixels. The telescopes are nominally separated by a distance of 80 m.

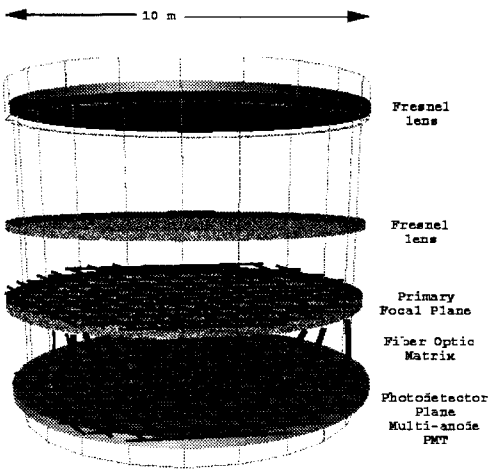

Figure 6: Conceptual Direct Cherenkov Observatory telescope structure. The UV transmitting Fresnel lenses provide the wide field of view (45-60°) for the instrument. Pixels in the focal plane are optically multiplexed to the photomultiplier readout plane to reduce cost.

the area surrounding the array. Additional considerations, such as field of view, also restrict the detection aperture. We note that the next generation of imaging Cherenkov telescope arrays, including VERITAS[21], HESS[22], and CANGAROO[23] begin to approach the strawman design, but with a substantially smaller field of view. These next generation gamma-ray imagers will likely be able to provide a proof of principle of the ability to measure DC light.

3.2. Charge Resolution

Above threshold, the DC light emission is independent of primary energy, making it an ideal measure of the primary charge. However, due to various background, detector resolution, and fluctuation processes, what one actually measures is not only the DC light emission, but rather the integrated DC light yield plus all background across the length of the primary cosmic track The charge resolution expected from the DC technique is therefore limited by a combination of various effects. In order to be conservative, we have assumed a detection scheme with an effective optical aperture of 100 m^2, a core location capability of 5 m, a time resolution of 6 ns, and an angular pixel size of 0.2°. Figure 9 shows the charge resolution expected resulting from these effects as a function of charge Z. For low charges the resolution is dominated by secondary Cherenkov light from the EAS. At higher Z the core resolution provides the charge resolution limitation. The overall resolution is calculated to be $\Delta Z/Z \sim 5\% \$ for $Z>10$, essentially independent of charge. We do not include the effects of optical or electronic signal multiplexing in this figure.

4.Other Science Goals

The DCO combination of high resolution charge measurement, sensitivity to cosmic rays in the PeV energy region, wide field-of view, and large detection aperture provides a wide range of new science opportunities.

4.1. *Measurement of Ultra-Heavy Nuclei (Z>26)*

The canonical theory of cosmic ray origin in the TeV to PeV energy region postulates origin of source material in supernova nucleosynthesis with subsequent shock-wave powered acceleration of this source material in the expanding shell of the supernova remnant. Accelerated cosmic rays propagate through the galactic magnetic field to the earth, with a propagation loss due to galactic escape and spallation off interstellar material depending on the pathlength from the source to the observation point. This model has been used to successfully model the observed energy spectra and mean elemental abundances from protons though iron up into the PeV energy regime.

The ultra heavy (UH) elements (Z>26) are thought to be created by r-process and s-process nucleosynthesis at supernova sites, and consequently they are expected to be present in the cosmic ray flux. Due to their high nuclear charge, these cosmic rays should be efficiently accelerated to higher energies than either proton or iron in a rigidity-limited acceleration mechanism. However, the flux of these particles in the PeV energy region is unknown due to the experimental difficulty in uniquely identifying these cosmic rays when using traditional, low resolution cosmic ray charge measurements. The presence of UH elements in the cosmic ray flux, and in particular the presence of a spectral break of these elements which is consistent with rigidity dependent spectral breaks in iron, carbon, and proton energy spectra, can provide a direct test of the universality of the rigidity-dependent particle acceleration process thought to be responsible for light element (Z<26) cosmic ray origin. Absence of such correlations may new sources of cosmic rays to be postulated for energies above the cosmic ray knee.

Figure 1 illustrates an estimate of the ultra-heavy nuclei flux based upon leaky-box model extrapolations[14] of lower energy satellite measurements[13]. At 1000 TeV energies, the UH flux is approximately 1/1000 of the iron flux. With a 2×10^4 m^2 sr detection aperture and 15% on-time, one expects to measure several UH nuclei/year with the DCO.

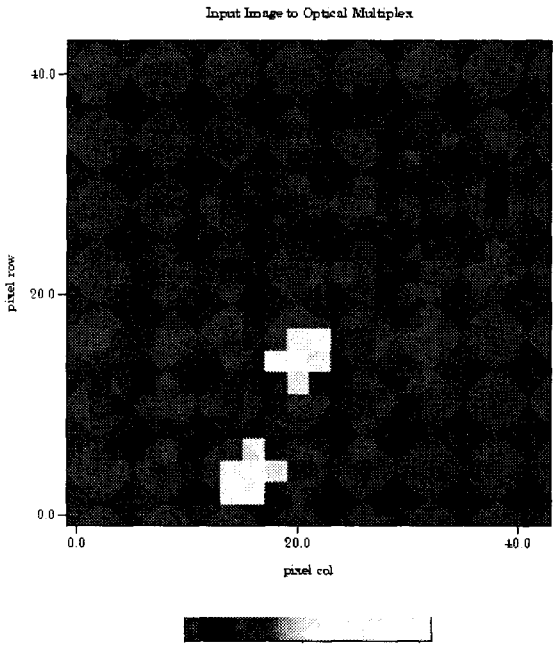

Figure 7: Simulated input image into multiplexed focal plane. Individual pixels are seeded with two Cerenkov images and a Gaussian low level background light. Simulation uses 1075 pixels read out by 150 multiplexed channels.

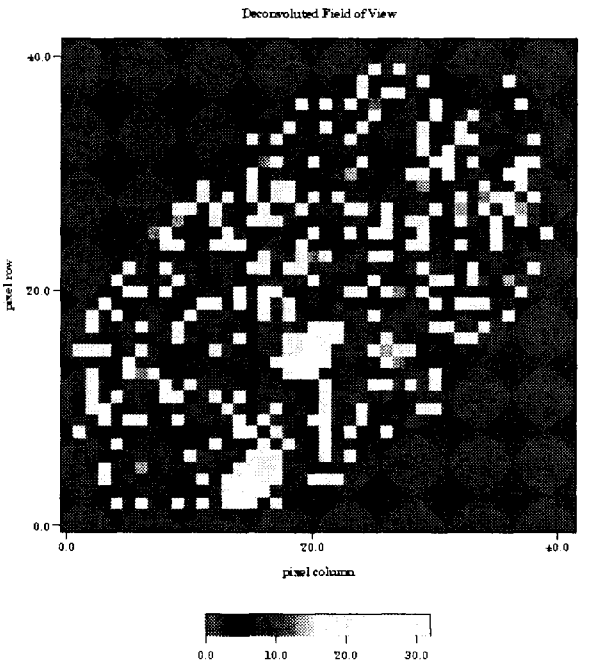

Figure 8: Deconvoluted focal plane image from150 channels of data generated by Figure 7 input image. The two original Cherenkov image are clearly resolved in the deconvoluted image.

with charge Z >> 100. A dedicated large aperture Direct Cherenkov observatory can serendipitously provide an excellent time-average and instantaneous all-sky sensitivity, creating a new capability for looking for transient sources of TeV gamma rays.

6. Acknowledgements

This work was partially supported under NSF Grant #PHY 0079704 and the Utah High Energy Astrophysics Institute.

7. References

1. A.R. Bell, *M.N.R.A.S.* **182**, 147 (1987).
2. A.R. Bell, *M.N.R.A.S.* **182**, 443 (1987).
3. R.D. Blanford and J.P.Ostriker, *Ap. J.* **221**, L29 (1978).
4. G.F. Krymsky, *Dokl. Akan. Nauk. USSR* **236**, 1306 (1977).
5. R. Schlickeiser, *Ap. J. Suppl.* **90**, 929 (1994).
6. P.O. Lagage and C.J. Cesarsky, *A&A* **125**, 249 (1983).
7. E. Juliusson, P. Meyer, and D. Müller, *Phys. Rev. Lett.* **29**, 445 (1972).
8. D. Kieda ,S..P. Swordy and S.P. Wakely, *Ap. Phys.* **15**, 287 (2001).
9. K. Sitte, *Proc. 9th ICRC (London)* **2**, 887 (1965).
10. M.P. Gough, *J. Phys. G:Nucl. Phys.* **2** (12) 965 (1976).
11. R.K. Sood, *Nature* **301**, 44 (1983).
12. D. Seckel *et al.,Proc. 26th ICRC (Salt Lake City)* **3**, 171 (1999).
13. W. R. Binns *et al.,Ap J.* **346**, 997 (1989).
14. S. P. Swordy, *Proc 24th ICRC, Rome, Italy* **2**, 697 (1995).
15. A.M. Hillas, *J. Phys. G: Nucl. Phys.* **G8**, 1461 (1982).
16. A.M. Hillas, *J. Phys. G: Nucl. Phys.* **G8**, 1475 (1982).
17. D.B. Kieda, *Ap. Phys.* **4**, 133 (1995).
18. D. Heck *et al., Forschungzentrum Karlsruhe Report FZKA* **6019**.
19. F. X. Kneizys *et al.,User's Guide to LOWTRAN 7, Hanscom AFB* **AFGL-TR-88-0177** (1988).
20. D. Lamb, *OWL/AIrwatch Optics Note \#UAH26OCT99* ,(http://owl.uah.edu/Papers/uah26oct99.PDF) (1999).
21. T.C. Weekes *et al., Ap. Phys.* **17**, 221 (2002).
22. W. Hofmann , in *GeV-TeV Gamma Ray Astrophysics Workshop (Snowbird, Utah 1999)* AIP **515**, 500 (2000).
23. M. Mori *et al.,* ibid, 485 (2000).
24. S. Banerjee et *al., J. Phys. G.* **25,** L15 (1999).
25. S. Banerjee et al., *Phys. Rev. Lett.* **85**, 1384 (2000).
26. J.J Drake *et al., Ap. J.* **572**, 996 (2002).
27. A. DeRujula, *Nucl. Phys. A***434**, 605 (1985).
28. J. Madsen, *hep-ph/0111417* (2001).
29. T.W. Kephart, and T. Weiler, *Ap. Phys.*, **4**, 271 (1996).
30. S.D. Wick *et al.,* submitted to *Ap. Phys. (astro-ph/0001233)* (2000).
31. R.C. Hartman *et al., Ap. J. Suppl.***123**, 79 (1999).
32. J. Gaidos *et al., Nature* **383**, 319 (1996).
33. G. Amelino-Camelia *et al., Nature* **383**, 319 (1998).
34. E. Witten, *Nucl. Phys. B***471**, 135 (1996).
35. S.D. Biller *et al., Phys. Rev. Lett.* **83**, 2108 (1999).